

Simple Spike Responses of Gaze Velocity Purkinje Cells in the Floccular Lobe of the Monkey During the Onset and Offset of Pursuit Eye Movements

R. J. KRAUZLIS AND S. G. LISBERGER

Department of Physiology, W. M. Keck Foundation Center for Integrative Neuroscience, and Neuroscience Graduate Program, University of California, San Francisco, California 94143

SUMMARY AND CONCLUSIONS

1. We recorded the simple spike firing rate of gaze velocity Purkinje cells (GVP-cells) in the flocculus/ventral paraflocculus of two monkeys during the smooth pursuit eye movements evoked by a target that was initially at rest, started suddenly, moved at a constant velocity, and then stopped.

2. For target motion in the preferred direction, GVP-cells showed a large transient increase in firing rate at the onset of pursuit, a smaller but sustained increase during the maintenance of pursuit, and a smooth return to baseline firing with little undershoot at the offset of pursuit. For target motion in the nonpreferred direction, GVP-cells showed a small decrease in firing rate at the onset of pursuit, a similar sustained decrease during the maintenance of pursuit, but a large transient increase in firing rate at the offset of pursuit before returning to baseline firing.

3. We pooled the data in our sample of horizontal GVP-cells by subtracting the population average of firing rate recorded during pursuit in the nonpreferred direction from the population average recorded during pursuit in the preferred direction. We transformed this net population average by passing it through a model of the brain stem final common pathway and the oculomotor plant. This yielded a signal that closely matched the observed trajectory of eye velocity during pursuit. We conclude that the transient overshoots exhibited in the firing rate of GVP-cells can provide appropriate compensation for the lagging dynamics of the oculomotor plant.

1990), possibly in parallel with activity mediated by other regions of the cerebellum, such as the oculomotor vermis and caudal fastigial nucleus (Büttner et al. 1991; Kase et al. 1979; Kurzan et al. 1993; Suzuki and Keller 1988a,b).

While a large number of studies have been devoted to the initiation, or onset, of pursuit, fewer have examined the mechanisms responsible for the termination, or offset, of pursuit. However, a number of recent studies have used a "step-ramp, step-stop" paradigm to investigate the trajectory of eye velocity at the offset of pursuit (Krauzlis and Lisberger 1994; Luebke and Robinson 1988; Rashbass 1961; Robinson et al. 1986). Because this paradigm provides roughly the same retinal image motion during the onset of pursuit in one direction as it does during the offset of pursuit in the other direction, it also provides a useful tool for analyzing the role of GVP-cells during pursuit. We report here that GVP-cells exhibit transient responses at the offset of pursuit in their nonpreferred direction, similar to the transient responses shown at the onset of pursuit in their preferred direction. If we assume that pursuit is driven reciprocally by GVP-cells from the two sides of the cerebellum, then the profiles of firing rate we have recorded form an appropriate command for eye velocity during both the onset and offset of pursuit.

INTRODUCTION

Pursuit eye movements rotate the eyes smoothly and slowly in the orbit to compensate for the motion of a visual target, thus minimizing the drift of the target's image across the retina (Westheimer and McKee 1975). The floccular lobe of the cerebellum, comprising the flocculus and ventral paraflocculus, represents an important node near the output of the pursuit system. Lesions of this structure in monkeys produce severe and permanent deficits in pursuit (Zee et al. 1981) and electrical stimulation produces smooth eye movements within 10 ms (Belknap and Noda 1987; Lisberger and Pavelko 1988; Shidara and Kawano 1993). In addition, gaze velocity Purkinje cells (GVP-cells) in the floccular lobe exhibit a large transient increase in their simple spike firing rate that coincides with the onset of visually elicited smooth eye movements (Shidara and Kawano 1993; Stone and Lisberger 1990). This activity is believed to reflect visual signals mediated by the floccular lobe that accelerate the eye at the onset of the smooth eye movement (Krauzlis and Lisberger 1991; Stone and Lisberger

METHODS

We recorded the activity of single GVP-cells in the floccular lobe of two monkeys, using methods that have been previously described (Stone and Lisberger 1990). Briefly, under halothane anesthesia and aseptic conditions, monkeys were implanted with a coil of wire in one eye for measuring eye movements (Judge et al. 1980), a head holder, and a recording cylinder. During experiments, monkeys sat in a specially designed primate chair with their head secured to the ceiling of the chair and faced a tangent screen onto which visual targets were projected. Extracellular potentials were recorded from P-cells with glass-insulated platinum-iridium microelectrodes while the monkeys tracked the visual targets in exchange for liquid reinforcements. In the present experiments, monkeys were trained to track the target motion illustrated in Fig. 1. The target was initially stationary, started suddenly to move at a constant velocity, and then stopped. At the onset of target motion, and again when the target stopped, a step displacement of the target was added to eliminate the need for the monkey to make corrective saccades. This target motion was randomly interleaved with other trials in which the target did not stop or in which its speed increased at an unexpected time. Only the record-

ings obtained during the step-ramp, step-stop trials are presented here.

For each GVP-cell, we aligned the responses on the onset of target motion and averaged the firing rate and eye velocity records from 20 to 30 trials. We then measured simple spike responses from the average firing rate profile. Examples of the intervals used for these measurements are shown in Fig. 2*A*. The initial resting rate (R_1) was measured as the average firing rate in the last 100 ms before the onset of target motion. The transient firing rate at the onset of pursuit (ON) was measured as the average firing rate over a 16-ms interval centered on the peak (or trough) in a time window from 50 to 300 ms after the onset of target motion. The transient response at the onset of pursuit was defined as the transient firing rate minus the initial resting rate ($ON-R_1$). The sustained firing rate (S) was measured as the average rate from 350 to 500 ms after the onset of target motion, and the sustained response for the onset of pursuit was defined as the sustained firing rate minus the initial resting rate ($S-R_1$). The transient firing rate at the offset of pursuit (OFF) was measured as the average firing rate over a 16-ms interval centered on the peak (or trough) in a time window 50 to 300 ms after the target stopped. The transient response at the offset of pursuit was defined as the transient firing rate minus the sustained firing rate ($OFF-S$). Finally, the postpursuit resting rate (R_2) was measured as the average firing rate over the last 100 ms of the trial, and the sustained response for the offset of pursuit was defined as the postpursuit resting rate minus the sustained firing rate (R_2-S).

RESULTS

We recorded from 20 Purkinje cells (6 from monkey 1, and 14 from monkey 2) that were classified as horizontal GVP-cells according to existing criteria (Lisberger and Fuchs 1978; Miles et al. 1980; Stone and Lisberger 1990). These cells showed strong modulation of firing rate during pursuit along the horizontal axis with the head stationary and weak modulation during pursuit along the vertical axis. Firing rate increased for eye motion toward the side of recording during pursuit and for head motion toward the side of recording during cancellation of the vestibulo-ocular reflex. We also recorded from 14 Purkinje cells (6 from monkey 1, and 8 from monkey 2) that showed an increase in firing rate during downward pursuit and a small increase during head motion away from the side of recording. The responses of vertical P-cells in the primate floccular lobe have not been examined during vertical head movements, but following a suggestion made previously (Stone and Lisberger 1990), we treated the 14 P-cells as the vertical equivalent of the horizontal GVP-cells.

Our basic finding was that the simple spike firing rate of GVP-cells showed a transient overshoot at the onset of pursuit in the preferred direction and at the offset of pursuit in the nonpreferred direction. Examples of the average simple spike firing rate recorded from four horizontal GVP-cells are shown in Fig. 1. At the onset of pursuit in the preferred direction (Fig. 1*A*), the simple spikes showed a sudden increase from the resting rate as eye speed increased from zero toward target speed. During the maintenance of pursuit in the preferred direction, when eye speed closely matched target speed, the firing rate was sustained at a level above resting rate but below the peak of the transient. Although in general it is common for eye velocity to overshoot target speed at the onset of pursuit (Krauzlis and Lisberger 1994; Luebke and Robinson 1988; Robinson et al. 1986), this

was not true of the behavior of the two monkeys in these experiments. The overshoots in firing rate at the onset of pursuit are therefore not a consequence of an overshoot in eye velocity. At the offset of pursuit (vertical dashed line), the firing rate decreased, but most of the GVP-cells did not show an undershoot before firing rate settled to a postpursuit resting rate at the end of the trial. The absence of an undershoot for most GVP-cells could not be attributed to clipping, because the firing rate usually remained well above zero (e.g., P-cell 3 in Fig. 1*A*). The postpursuit resting rate often differed slightly from that measured before the onset of pursuit, presumably because of the weak sensitivities of GVP-cells to eye position. At the onset of pursuit in the nonpreferred direction (Fig. 1*B*), the simple spikes showed a decrease from the resting rate as eye speed increased toward target speed. During the maintenance of pursuit in the nonpreferred direction, the firing rate remained at a level below resting rate similar to that reached at the onset of pursuit. At the offset of pursuit (vertical dashed line), the firing rate showed a sudden increase to a level above resting rate, remained at this elevated level as eye speed returned to zero, and then settled to a postpursuit resting rate at the end of the trial.

The responses of both the horizontal and vertical GVP-cells are summarized quantitatively in Fig. 2. For each GVP-cell, we used procedures outlined in the METHODS to measure the amplitudes of the transient and sustained changes in firing rate at the onset and offset of pursuit. We then plotted the amplitude of the transient response against the amplitude of the sustained response for each GVP-cell for the onset (Fig. 2*B*) and offset (Fig. 2*C*) of pursuit. In Fig. 2*B*, the circles plot above the line of slope one, indicating that the transient increase in firing tended to be larger than the sustained increase at the onset of pursuit in the preferred direction. The squares plot slightly below the line, indicating that the transient decrease in firing showed a similar but less pronounced tendency to be larger than the sustained decrease at the onset of pursuit in the nonpreferred direction. In Fig. 2*C*, the squares plot above the line, indicating that the transient increase in firing rate tended to be larger than the sustained increase at the offset of pursuit in the nonpreferred direction. The circles plot slightly below the line, indicating that the transient decrease in firing showed a similar but smaller tendency to be larger than the sustained decrease at the offset of pursuit in the preferred direction. Overall, the transient responses were most prominent at the onset of pursuit in the preferred direction and at the offset of pursuit in the nonpreferred direction, the two conditions associated with image motion in the preferred direction and with sudden increases in firing rate.

For the horizontal GVP-cells, we computed the average firing rate across the population at each millisecond of the trial. Figure 3 shows this population average during pursuit in the preferred (Fig. 3*A*) and nonpreferred directions (Fig. 3*B*) superimposed on the averaged eye velocity. As expected from inspection of individual GVP-cells, the average shows a transient overshoot at the onset of pursuit in one direction (Fig. 3*A*), as well as at the offset of pursuit in the opposite direction (Fig. 3*B*). However, unlike the behavior of most individual GVP-cells (Fig. 1), the average also shows a smooth decrease at the offset of pursuit that corre-

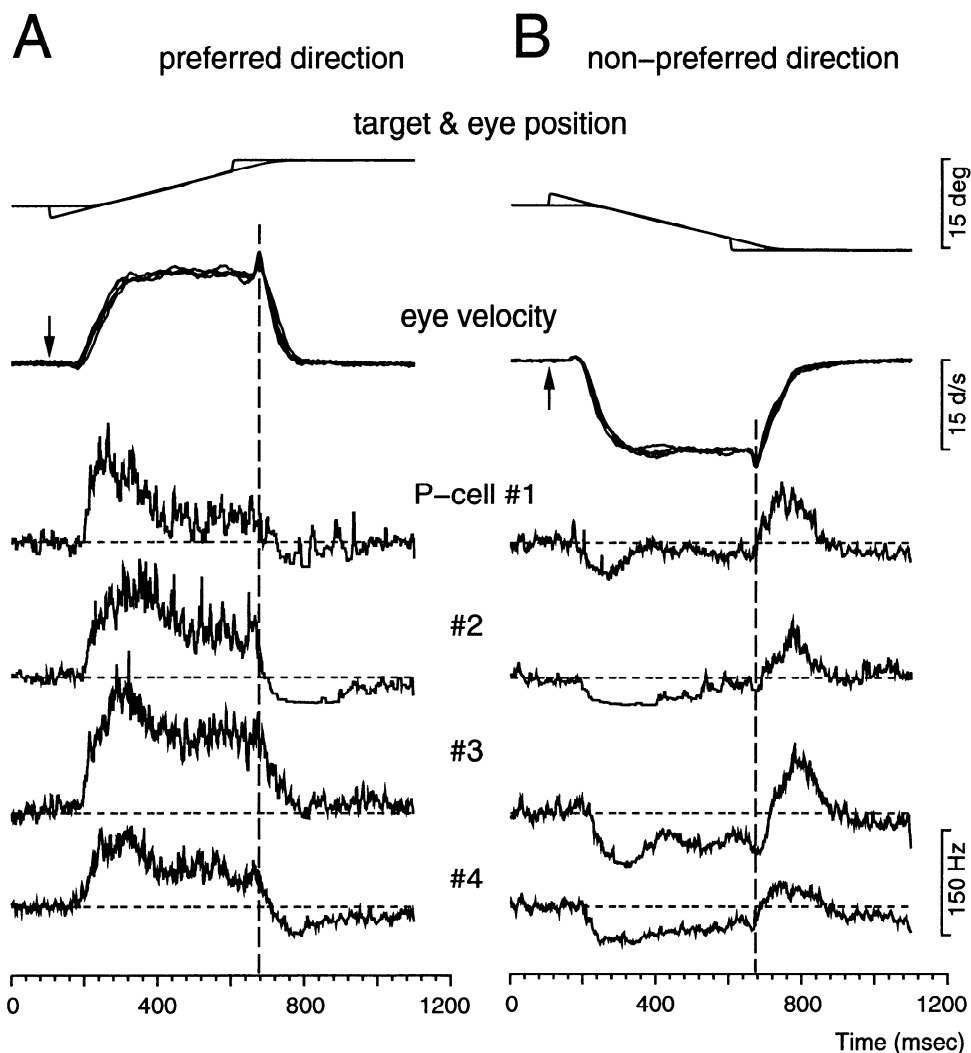


FIG. 1. Examples of average simple spike firing rate of gaze velocity Purkinje cells (GVP-cells) during the onset and offset of pursuit. *A*: pursuit in the preferred direction. *B*: pursuit in the nonpreferred direction. *Top traces*: average eye position superimposed on target position. Target motion started at 100 ms (indicated by arrows) and stopped at 600 ms. Superimposed eye velocity traces show the average eye velocity records obtained while recording from the 4 GVP-cells whose average firing rate is shown below. Dashed vertical lines mark the beginning of the offset of pursuit. Dashed horizontal lines indicate the resting rate for each GVP-cell; these resting rates were 73 (#1), 44 (#2), 85 (#3), and 85 spikes/s (#4). All 4 cells were identified as horizontal GVP-cells.

sponds closely to the decrease in eye speed (Fig. 3*A*). The time constant of the decay in the population average of firing rate is the same as the time constant of the decay in eye velocity ($\tau = 64$ ms). At the same time during pursuit in the nonpreferred direction (Fig. 3*B*), the population average shows a matching exponential rise ($\tau = 67$ ms). The *inset* (Fig. 3*A*) illustrates that the average firing rate also shows a small transient increase that precedes a similar increase in eye velocity by 12 ms. This transient change in eye velocity was presumably caused by the step displacement introduced when the target was stopped. Under the assumption that horizontal eye velocity is driven reciprocally by two lateralized populations of horizontal GVP-cells with opposite directional preferences, we next determined a bilateral population average by subtracting the average firing rate during pursuit in the nonpreferred direction (Fig. 3*B*) from that during pursuit in the preferred direction (Fig. 3*A*). As shown in Fig. 3*C*, this bilateral population average of horizontal GVP-cell firing rate shows an undershoot as pursuit stops that complements the overshoot seen as pursuit starts.

We next asked how this population average (Fig. 3*C*) would have to be transformed to create the eye velocity measured at the same time. The population average of firing rate was used as the input to the brain stem and eye

plant model shown schematically in Fig. 3*D* and described in the APPENDIX. We set all parameters of the model equal to published values, except for the gains (G_p , G_i , and G_s) in the pathways of the "brain stem final common pathway". These three parameters were adjusted to produce the least squares best fit shown in Fig. 3*E* between the model eye velocity and that measured during our recordings. The fit is not exact, in particular, the predicted eye velocity lags actual eye velocity by several milliseconds, but the overshoot and undershoot evident in the population average (Fig. 3*C*) are not present in the model output, and the slope of measured eye velocity is closely matched by the model output during the onset and offset of pursuit. The optimal fit in Fig. 3*E* was obtained when the gain for the "step" pathway was much higher ($G_i = 1.18$), than the gains for either the "pulse" ($G_p = 0.03$) or "slide" ($G_s = 0.02$) pathways. This indicates that a simple integration of horizontal GVP-cell firing was nearly sufficient to produce a pattern of motoneuron firing that would result in the model output shown in Fig. 3*E*.

DISCUSSION

We have shown that GVP-cells in the floccular lobe of the monkey show transient responses at the offset of pursuit in their nonpreferred direction, as well as at the onset of

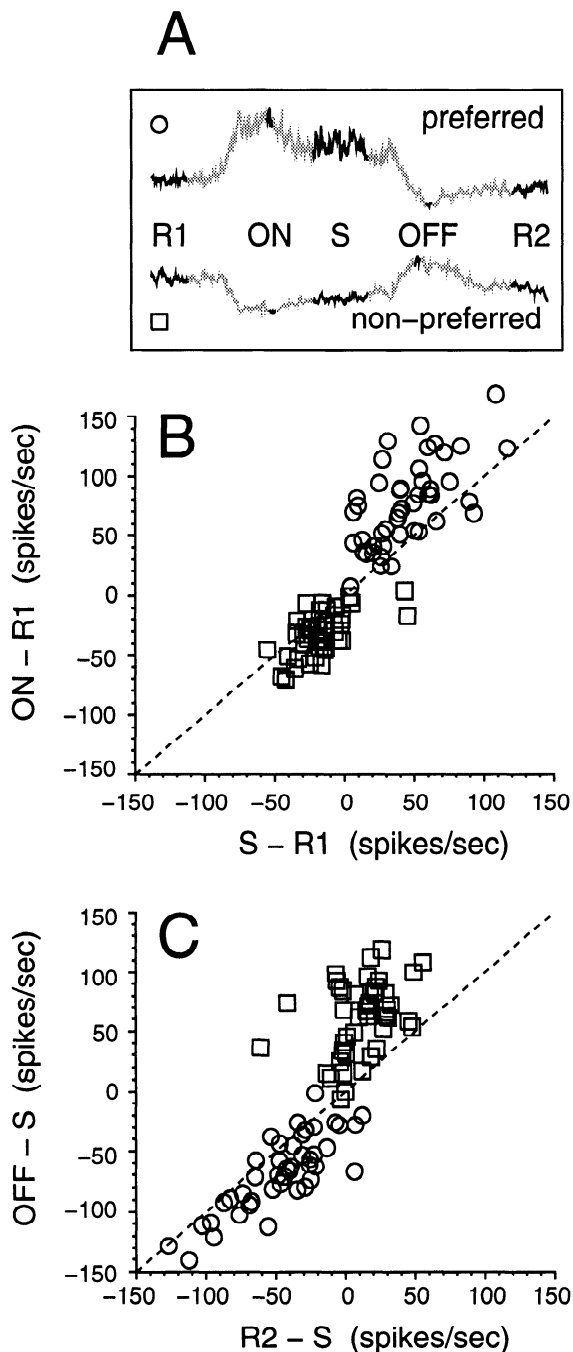


FIG. 2. Quantitative comparison of transient and sustained responses of GVP-cells during the onset and offset of pursuit. *A*: schematic diagram illustrating how the measurements were made for 1 GVP-cell. Abbreviations: R_1 , initial resting rate; ON, transient firing rate at the onset of pursuit; S, steady-state firing rate during maintained pursuit; OFF, transient firing rate at the offset of pursuit; R_2 , final resting rate. *B*: transient response plotted against sustained response for measurements taken from the onset of pursuit. *C*: transient response plotted against sustained response for measurements taken from the offset of pursuit. Each symbol represents a measurement from one GVP-cell. Circles show measurements taken during pursuit in the preferred direction; squares during pursuit in the nonpreferred direction. The dashed oblique lines indicate slopes of one.

pursuit in their preferred direction. This result indicates that while eye velocity at the offset of pursuit often does not show the overshoot and ringing characteristic of the onset of pursuit (Krauzlis and Lisberger 1994; Luebke and Robin-

son 1988; Robinson et al. 1986), eye velocity may be driven downward to zero at the offset of pursuit by the same mechanism that drives it upward to target speed at the onset of pursuit.

Previous studies have simulated the firing rate of floccular GVP-cells using as inputs a weighted sum of signals related to pursuit eye movements and visual inputs (Krauzlis and Lisberger 1991; Shidara et al. 1993). These approaches have shown that combinations of sensory and kinematic variables can account for GVP-cell firing, but they have not shown that the corollary relationship is true, namely, that GVP-cell firing can drive the observed eye movements. Here, we have examined the suitability of GVP-cell firing as a command for eye movement by simulating the pursuit eye movement that results when average GVP-cell firing rate is provided as an input to the brain stem oculomotor pathways. We have demonstrated that mathematical integration of the activity of horizontal GVP-cells produces a signal that, when passed through a model of the oculomotor plant, nearly reproduces the observed trajectory of pursuit eye velocity. This suggests that the transient overshoots in GVP-cell firing rate may provide the pre-emphasis needed to compensate for the lagging dynamics of the oculomotor plant during pursuit (Robinson 1965), analogous to the role burst neurons in the pontine reticular formation fulfill for saccadic eye movements (Gisberger et al. 1981).

Study of saccadic eye movements has demonstrated that an additional "slide" component in the neural innervation is necessary to compensate for a lead element in the plant dynamics (Optican and Miles 1985). Previous papers have assumed that the slide component of the neural innervation is provided by circuitry within the brain stem. Our results suggest that for pursuit eye movements, this component may be included in the population average of GVP-cell firing rate, since the best match between the model output and recorded eye velocity was obtained when the gain of the slide brain stem pathway (G_s) was very small. In addition, the time constants we measured in the population average of GVP-cell firing rate (Fig. 3, *A-B*) lie within the range of values associated with this slide component (Goldstein 1983). Our data therefore suggest either 1) that the final brain stem pathways for pursuit eye movements are only partly shared with those for saccades or 2) that the slide component of saccadic innervation arises outside the final brain stem pathways.

APPENDIX

The bilateral population average firing rate plotted in Fig. 3C was first delayed by 9 ms to duplicate the transmission delays observed with electrical stimulation of the flocculus (Lisberger and Pavclko 1988; Shidara and Kawano 1993). The delayed firing rate was then provided as an input to the proposed brain stem compensatory network, or "brain stem final common pathway" (Optican and Miles 1985). This portion of the model consisted of three limbs, as shown in Fig. 3D. The "pulse" limb transmitted the delayed firing rate scaled by a gain, G_p . The "step" limb integrated the delayed firing rate and scaled it by G_i . Finally, the "slide" pathway low-pass filtered the delayed firing rate and scaled it by G_s . The time constant of the slide ($T_s = 80$ ms) was based on the observed decay in motoneuron firing rate in the immediate wake of saccadic eye movements (Goldstein 1983). The three gains in this description of the brain stem pathways ($G_i = 1.18$, $G_p = 0.03$, and $G_s = 0.02$) were the fitted parameters of our model.

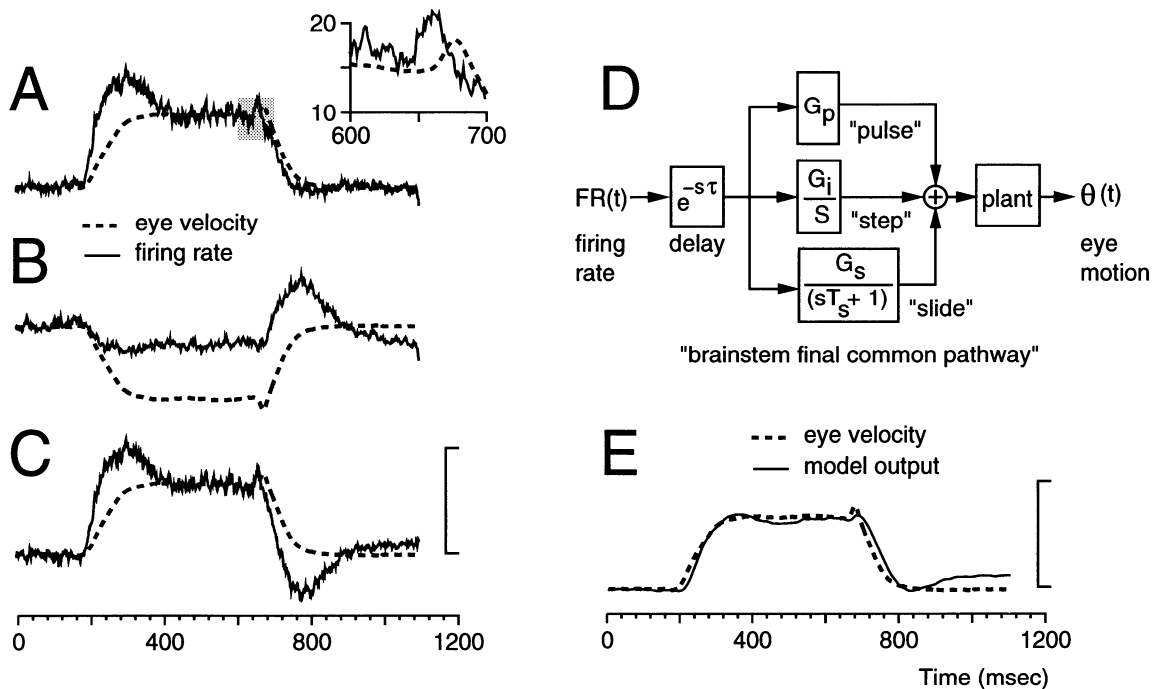


FIG. 3. Population average of the firing rate of 20 horizontal GVP-cells and the effects of transforming it with a model of the brain stem and oculomotor plant. *A*: solid trace shows the population average of firing rate during pursuit in the preferred direction. Dashed trace shows average eye velocity. Target motion (not shown) started at 100 ms and stopped at 600 ms. *B*: solid trace shows population average during pursuit in the nonpreferred direction. Dashed trace shows average eye velocity. *C*: solid trace shows the result of subtracting the population average of firing rate for target motion in the nonpreferred direction from that for target motion in the preferred direction. Dashed trace shows average eye velocity. The vertical scale indicates 25 deg/s for eye velocity in *A-C*, and 77, 77, and 97 spikes/s for firing rate in *A*, *B*, and *C*, respectively. *D*: model of the brain stem and oculomotor plant used to transform average GVP-cell firing rate. The fitted model parameters were $G_i = 1.18$, $G_p = 0.03$, and $G_s = 0.02$. Details of the model are provided in the APPENDIX. *E*: solid trace shows the result of passing the firing rate shown by the solid trace in *C* through the model shown in *D*. Dashed trace shows average eye velocity. The vertical scale indicates 25 deg/s.

For comparison, the gains used to fit the saccadic data of Optican and Miles (1985) were $G_i = 1.00$, $G_p = 0.24$, and $G_s = 0.057$ (L. Optican, personal communication).

The sum of the outputs of the three brain stem pathways provided the neural innervation presumed to be applied by motoneurons as an input to the oculomotor plant. Our model of the oculomotor plant followed Robinson's linear fourth-order description for human eye movements (Robinson 1964) but with the parameters changed as suggested previously (Fuchs et al. 1988) to describe monkey eye movements. The neural innervation (FR) was converted to active state tension (F_o) with the equation

$$F_o = \frac{K_T}{K_S} FR$$

where $K_T = 1.0 \text{ g/deg}$ and $K_S = 4.3 \text{ s} \cdot \text{s}^{-1} \text{ deg}^{-1}$.

Muscle force (F_m) was obtained from active state tension (F_o) using the following differential equation describing muscle dynamics

$$\frac{R_m}{K_e} \dot{F}_m + F_m = F_o - R_m \dot{\theta}$$

where $R_m = 0.04 \text{ g} \cdot \text{d}^{-1} \cdot \text{s}^{-1}$ and $K_e = 4 \text{ g/d}$.

Finally, F_m was applied to the orbit, orbital tissues, and passive muscle, modeled as two Voigt elements connected in series

$$\frac{\theta(s)}{F_m(s)} = \frac{1}{K_T} \frac{(1 + T_3s)}{(1 + T_1s)(1 + T_2s)}$$

where $T_1 = 0.012 \text{ s}$, $T_2 = 0.260 \text{ s}$, $T_3 = 0.140 \text{ s}$, and $K_T = 1.0 \text{ g/deg}$.

We obtained nearly identical results using a simpler model that

did not include a description of muscle force or muscle dynamics. In this simpler model, the neural innervation was applied directly to a second-order model of the oculomotor plant described by two real poles ($T_1 = 160 \text{ ms}$, $T_2 = 16 \text{ ms}$) and a zero ($T_z = 80 \text{ ms}$). In general, studies of the oculomotor plant have mostly examined the dynamics of saccadic eye movements; it is therefore uncertain whether available estimates of the time constants of the plant provide an accurate description of plant behavior during slow eye movements. Measurements of force generated during pursuit eye movements in humans (Robinson 1965) indicates that an additional pole ($T = 500 \text{ ms}$) may be necessary to adequately model the impact of viscous elements on the dynamics of slow eye movements, but we have not tested the more complex plant model suggested by this observation.

We are grateful to Drs. Frederick Miles and Lance Optican for many helpful discussions.

This research was supported by National Eye Institute Grant EY-03878.

Address for reprint requests: R. J. Krauzlis, Lab. of Sensorimotor Research, National Institutes of Health, Bldg. 49, Rm. 2A-50, Bethesda, MD 20892.

Received 14 June 1994; accepted in final form 27 July 1994.

REFERENCES

BELKNAP, D. B. AND NODA, H. Eye movements evoked by microstimulation in the flocculus of the alert macaque. *Exp. Brain Res.* 67: 352-362, 1987.
 BÜTTNER, U., FUCHS, A. F., MARKERT-SCHWAB, G., AND BUCKMASTER, P. Fastigial nucleus activity in the alert monkey during slow eye and head movements. *J. Neurophysiol.* 65: 1350-1371, 1991.

- FUCHS, A. F., SCUDDER, C. A., AND KANEKO, C. R. S. Discharge patterns and recruitment order of identified motoneurons and internuclear neurons in the monkey abducens nucleus. *J. Neurophysiol.* 60: 1874–1895, 1988.
- GISBERGEN, J. A. M. VAN, ROBINSON, D. A., AND GIELEN, S. A quantitative analysis of generation of saccadic eye movements by burst neurons. *J. Neurophysiol.* 45: 417–442, 1981.
- GOLDSTEIN, H. P. *The neural encoding of saccades in the rhesus monkey* (PhD thesis). Baltimore, MD: Johns Hopkins Univ., 1983.
- JUDGE, S. J., RICHMOND, B. J., AND CHU, F. C. Implantation of magnetic search coils for measurement of eye position: an improved method. *Vision Res.* 20: 535–538, 1980.
- KASE, M., NODA, H., SUZUKI, D. A., AND MILLER, D. C. Target velocity signals of visual tracking in vermal Purkinje cells of the monkey. *Science Wash. DC* 205: 717–720, 1979.
- KRAUZLIS, R. J. AND LISBERGER, S. G. Visual motion commands for pursuit eye movements in the cerebellum. *Science Wash. DC* 253: 568–571, 1991.
- KRAUZLIS, R. J. AND LISBERGER, S. G. Temporal properties of visual motion signals for the initiation of smooth pursuit eye movements in monkeys. *J. Neurophysiol.* 72: 150–162, 1994.
- KURZAN, R., STRAUBE, A., AND BÜTTNER, U. The effect of muscimol micro-injections into the fastigial nucleus on the optokinetic response and the vestibulo-ocular reflex in the alert monkey. *Exp. Brain Res.* 94: 252–260, 1993.
- LISBERGER, S. G. AND FUCHS, A. F. Role of primate flocculus during rapid behavioral modification of vestibuloocular reflex. I. Purkinje cell activity during visually guided horizontal smooth-pursuit eye movements and passive head rotation. *J. Neurophysiol.* 41: 733–777, 1978.
- LISBERGER, S. G. AND PAVELKO, T. A. Brain stem neurons in modified pathways for motor learning in the primate vestibulo-ocular reflex. *Science Wash. DC* 242: 771–773, 1988.
- LUEBKE, A. E. AND ROBINSON, D. A. Transition dynamics between pursuit and fixation suggest different systems. *Vision Res.* 28: 941–946, 1988.
- MILES, F. A., FULLER, J. H., BRAITMAN, D. J., AND DOW, B. M. Long-term adaptive changes in primate vestibuloocular reflex. III. Electrophysiological observations in flocculus of normal monkeys. *J. Neurophysiol.* 43: 1437–1476, 1980.
- OPTICAN, L. M. AND MILES, F. A. Visually induced adaptive changes in primate oculomotor control signals. *J. Neurophysiol.* 54: 940–958, 1985.
- RASHBASS, C. The relationship between saccadic and smooth tracking eye movements. *J. Physiol. Lond.* 159: 326–338, 1961.
- ROBINSON, D. A. The mechanics of human saccadic eye movement. *J. Physiol. Lond.* 174: 245–264, 1964.
- ROBINSON, D. A. The mechanics of human smooth pursuit eye movement. *J. Physiol. Lond.* 180: 569–591, 1965.
- ROBINSON, D. A., GORDON, J. L., AND GORDON, S. E. A model of the smooth pursuit eye movement system. *Biol. Cybern.* 55: 43–57, 1986.
- SHIDARA, M. AND KAWANO, K. Role of Purkinje cells in ventral paraflocculus in short-latency ocular following responses. *Exp. Brain Res.* 93: 185–195, 1993.
- SHIDARA, M., KAWANO, K., GOMI, H., AND KAWATO, M. Inverse-dynamics model eye movement control by Purkinje cells in the cerebellum. *Nature Lond.* 365: 50–52, 1993.
- STONE, L. S. AND LISBERGER, S. G. Visual responses of Purkinje cells in the cerebellar flocculus during smooth-pursuit eye movements in monkeys. I. Simple spikes. *J. Neurophysiol.* 63: 1241–1261, 1990.
- SUZUKI, D. A. AND KELLER, E. L. The role of the posterior vermis of monkey cerebellum in smooth-pursuit control. I. Eye and head movement related activity. *J. Neurophysiol.* 59: 1–18, 1988a.
- SUZUKI, D. A. AND KELLER, E. L. The role of the posterior vermis of monkey cerebellum in smooth-pursuit control. II. Target velocity related Purkinje cell activity. *J. Neurophysiol.* 59: 19–40, 1988b.
- WESTHEIMER, G. AND MCKEE, S. P. Visual acuity in the presence of retinal-image motion. *J. Opt. Soc. Am.* 65: 847–850, 1975.
- ZEE, D. S., YAMAZAKI, A., BUTLER, P. H. AND GÜCER, G. Effects of ablation of flocculus and paraflocculus on eye movements in primate. *J. Neurophysiol.* 46: 878–899, 1981.